Pergamon

PII: S0191–8141(97)00111–9

Journal of Structural Geology, Vol. 20, No. 5, pp. 601 to 615, 1998

0191-8141/98 $19.00 + 0.00

Criteria for incipient slaty and crenulation cleavage development in Tertiary flysch of the Helvetic zone of the Swiss Alps

HANAN J. KISCH

Department of Geological and Environmental Sciences, Ben-Gurion University of the Negev, P.O. Box 653, Beer-Sheva 84 105, Israel

(*Received* 21 *January* 1997; *accepted in revised form* 17 *November* 1997)

Abstract—Two parameters of incipient cleavage development are compared in a series of Tertiary flysch from the Helvetic zone of the Swiss Alps: (1) the overall relative phyllosilicate orientation as obtained from the X-ray diffraction intensity ratio of their 00l reflections in cleavage- and bedding-parallel slabs ($I_{10Å\ (0.5°)}$ C/B) and (2) the dimensional aspect ratios of fissility fragments, the 'cleavage/bedding fissility ratio' (c/b).

These two parameters show a roughly linear power relationship with a wide scatter. Appreciably better fits are obtained if populations showing different cleavage morphology (closely vs widely spaced cleavage; crenulation vs non-crenulation cleavage) and lithology (silt and fine-sand size quartz content; carbonate content) are plotted separately. In contrast, there is no clear link between the two criteria of cleavage intensity and the degree of incipient metamorphism as expressed by illite 'crystallinity'.

Samples with crenulation cleavage show both lower ($I_{10Å\ (0.5°)}$ C/B) and c/b cleavage/bedding fissility ratios than most of those with non-crenulation domainal cleavages with closely spaced cleavage domains; these lower ratios reflect the presence of an earlier, largely bedding-parallel, cleavage fabric. This difference in the ratios between these groups of cleavage morphologies proves that the cleavage/bedding fissility ratio is not only dependent on the overall phyllosilicate orientation, but also on the cleavage microstructure, in particular the morphology and spacing of the cleavage domains and the persistence of a bedding-parallel cleavage fabric in the microlithons of the crenulated samples. The relationship between the c/b cleavage/bedding fissility ratio and the $I_{10Å\ (0.5°)}$ C/B ratio can provide a useful indication of the type of incipient cleavage fabric developed, and help in detecting the presence of an earlier slaty cleavage. Additional measurement of the intersection/bedding fissility ratio i/b on the fissility fragments is likely to help in assessing the effect of lithology, particularly the effect of the initial bedding anisotropy.

The differences in the illite/chlorite ratios in the cleavage and bedding planes, as determined from the $I_{10Å}/I_{7Å}$ C/B ratio, provides information regarding the relative formation of illite and chlorite in the cleavage domains and the chlorite–mica 'stacks' during development of the cleavage fabric. © 1998 Elsevier Science Ltd. All rights reserved

INTRODUCTION

Attempts to relate the intensity of bedding- and cleavage-parallel fissility or quality of parting to degree of phyllosilicate orientation are of venerate standing—Sorby (1853) in slates; Ingram (1953) in mudrocks (see also references in Groshong, 1988, p. 1332). In earlier studies, the degree of orientation was qualitatively assessed by microscopy.

Since the 1970s several studies have used X-ray texture goniometry (pole figures) to quantitatively assess the degree of phyllosilicate orientation in relation to strain (Oertel, 1983) and to mechanisms of phyllosilicate reorientation in sequences of progressive cleavage development (Holeywell and Tullis, 1975; Ho *et al.*, 1995, 1996 and references therein). However, this technique, although admittedly more quantitatively three dimensional, is time-consuming and not universally available.

XRD intensity ratios on C- and B-parallel slabs

In an earlier paper the writer developed a simple X-ray diffraction method to assess the relative orientation of phyllosilicate minerals in the cleavage (C) and the bedding (B) directions in samples with an appreciable cleavage–bedding angle (Kisch, 1994). The method uses the ratios of the intensities of the basal X-ray reflections of these minerals as measured on slabs cut parallel to the C and B planes, using a divergence/scatter slit set of 0.5°. For the mica-type phyllosilicates a 10 Å reflection is used, and the ratio of their intensities in the C- and B-parallel slabs is hence referred to as the $I_{10Å\ (0.5°)}$ C/B intensity ratio. The method is essentially a 'poor man's method' to determine the total phyllosilicate microfabric. In addition, the intensity ratios of the basal reflections of different phyllosilicate minerals give information on differences between phyllosilicate proportions in the C- and B-parallel slabs, for instance the $I_{10Å}/I_{7Å}$ intensity ratio on the mica/chlorite ratio.

Provisional high-resolution X-ray texture goniometry (HRXTG) work was carried out by van der Pluijm at the University of Michigan, Ann Arbor, on five samples from the Caledonides of Jämtland (western central Sweden), using the transmission-mode methods described by van der Pluijm *et al.* (1994). This yielded orientation parameters showing good qualitative correspondence with the C/B 10 Å XRD intensity ratios for four of the samples. A more extensive study of the re-

lation between the different orientation parameters is being planned.

The c/b cleavage/bedding fissility ratio

A field classification and intensity scale for cleavages has been developed by Durney and Kisch (1994). It is based on the cleavage/bedding fissility ratio (hence the c/b ratio) as quantified by measurement of the dimensional aspect ratios of fissility fragments in the cleavage direction relative to the bedding direction—i.e. along the planes of cleavage- and bedding-fabric anisotropy—in the plane normal to the bedding/cleavage intersection, and represents the intensity of cleavage fissility relative to bedding fissility in the same sample.

The $I_{10Å\ (0.5°)}$ C/B ratios reflect the relative phyllosilicate orientation parallel to cleavage only, whereas the cleavage fabric anisotropy, and therefore the cleavage/bedding fissility ratios, must reflect additional microstructural characteristics, such as the presence and shape of cleavage domains, and lithology. The two parameters, therefore, cannot be expected to show a strictly linear relationship, and it is of interest to evaluate to what extent they correlate, and whether the lack of correlation provides evidence on the microstructure.

The phyllosilicate orientation as obtained from the XRD method was compared to the field classification and intensity scale for cleavages for a suite of rocks from the Caledonides of Jämtland. An attempt was made to interpret the appreciable differences between the cleavage intensity as obtained by these two methods in terms of differences of the microfabric. It was concluded that the common combination of relatively good cleavage/bedding fissility ratios of 0.67 and 3 with poor $I_{10Å\ (0.5°)}$ C/B ratios of less than unity can be related to the development of discrete crenulation cleavages or domainal cleavages with little C-parallel mica orientation either in the microlithons or the cleavage domains.

The i/b intersection/bedding fissility ratio

As the c/b ratio shows the *relative* degree of cleavage development compared with bedding fabric, and incorporates effects due to the initial bedding anisotropy, differences in this ratio are, in part, due to differences in initial bedding anisotropy. In order to indicate the extent of tectonic fabric development in rocks of *different* initial bedding anisotropy, an additional i/b intersection/bedding fissility ratio was adopted by Durney and Kisch: "i/b represents an index for the degree of directional tectonic fabric development which begins at the most incipient stages [and] for this reason should be closely related to the degree of tectonic deformation" (Durney and Kisch, 1994, p. 272).

On the logarithmic three-axis grid for plotting c/b and i/b fissility ratios introduced by Durney and Kisch (1994, fig. 6) (cf. Fig. 9), the three-dimensional fissility-fragment shapes of a cleavage–fissility series of mudstones with a similar lithology from the Manilla district, New South Wales, Australia, are distributed in an I-constant band parallel to the c/b axis—the 'Manilla mudstone field' (Durney and Kisch, 1994, fig. 12). As the tectonic deformation style that gave rise to these cleavages was similar, this feature reflects the similar initial bedding fabrics; the strong initial bedding/cleavage fissility ratio $b_0/c_0 = 6.3$, a measure of this initial anisotropy, is obtained by projecting the samples back to the -C axis (or $i/b = 1$ axis). Rocks with significantly higher bedding anisotropies occupy a parallel 'shale field', at lower c/b ratios for similar i/b ratios, and a much higher initial bedding anisotropy b_0/c_0 of 30–50 (Durney and Kisch, 1994, p. 220 and fig. 15).

The i/b ratio thus gives information on the degree of tectonic fabric development in any one lithology and structural/tectonic regime. Unfortunately, i/b was only measured for some of the samples because at the time of sampling its relevance was not apparent.

The purpose of this paper is to investigate the relationship between the cleavage intensities as expressed by the two methods in a suite of slates and slaty mudstones of mid-anchimetamorphic to 'diagenetic' grade from Tertiary flysch of the Helvetic zone of the Swiss Alps, and to relate the differences to the lithology and microfabric of these rocks.

SAMPLES STUDIED

Samples were collected from Tertiary flysch of the Helvetic realm, largely from localities from which the illite 'crystallinities' had earlier been studied by Kisch (1980). The sampling localities can be divided in three groups, from northeast to southwest

1. Linthal–Urnerboden–upper Schächental–Trübsee;
2. Gasperini quarry near Attinghausen–Seedorf (Reuss Valley); and
3. Kandertal, La Tièche and Diablerets area.

The samples from areas (1) and (2) are from the Infrahelvetic complex (Milnes and Pfiffner, 1977; Pfiffner, 1978), which "encompasses all units underlying the Glarus overthrust" (the basal thrust of the Helvetic nappe system), including the exotic ultrahelvetic and allochthonous subhelvetic units and the underlying autochthonous–parautochthonous flysch; most are from the subhelvetic Griesstock nappe and the North-Helvetic Flysch.

Crenulation cleavage is common in the Linthal–Urnerboden–Schächental. Milnes and Pfiffner (1977; also Pfiffner, 1978) noted that the regional penetrative foliation in the Infrahelvetic complex "is affected in irregular patches by small-scale crenulations often accompanied by a well-developed crenulation cleavage" (1977, p. 89). They attributed the penetrative cleavage

to the Calanda deformation phase of probably Late Oligocene age, and the superimposed crenulation cleavage to the last Helvetic deformation phase, related to movements along the basal Helvetic thrust (Glarus overthrust), the Ruchi phase of mid-Miocene age. However, "structural correlation on the basis of style is a hazardous procedure in this region" (Milnes and Pfiffner, 1977, p. 90), and "there is no argument for a specific time of non-deformation between the Calanda and Ruchi phases" (Milnes and Pfiffner, 1977, p. 89).

The samples from area (3) are largely of flysch of the Helvetic nappe system proper, mainly of the lower-Helvetic Morcles nappe (e.g. southeast of Solalex), the middle-Helvetic Diablerets–Gellihorn nappe (e.g. Kandergrund) and the Ultrahelvetic Plaine–Morte nappe (e.g. northeast of Taveyanne; Creux de Culan, south of Diablerets; south of Lac de Derborence).

These sampling localities are listed in Table 1 and shown on Fig. 1.

The metamorphic grades as determined from illite 'crystallinity' are largely mid- to high-anchimetamorphic for the first area, with low-anchimetamorphic to high-'diagenetic' grades for two localities; for the other two areas the grades are almost exclusively 'diagenetic'.

MICROFABRICS

A brief summary of the lithology and cleavage type of the investigated samples is given in Table 1.

(1) Linthal–Urnerboden–upper Schächental–Trübsee

The typical Dachschiefer at Linthal, Chlus and Wanneler Bach are fine-silty shales (less than 25% silt-size clasts) and mudstones showing a smooth incipient crenulation cleavage, visible even when the angle between cleavage and bedding is as small as 15° (e.g. Z91-8 and Z91-9). The domains are spaced some 50–100 μm and have a high continuity, but typically constitute only $<10\%$ of the slate volume. The crenulation cleavage is predominantly discrete, but in many samples the micas in the outer margins of the microlithons locally show a strong cleavage-parallel deflection into the cleavage domains, giving the latter diffuse and frayed boundaries ('zonal' crenulation cleavage); locally clastic micas continue through the crenulation-cleavage domains with angles of up to 25° to the cleavage. The fabric being crenulated is a marked penetrative slaty cleavage, bedding-parallel in most samples.

It should be noted that 'zonal' is used here as a morphologic variety of crenulation cleavage in the original sense of Gray (1977a,b; also Powell, 1979) as the opposite of 'discrete' crenulation cleavage: "the cleavage is a zone and has diffuse somewhat arbitrary boundaries through which the initial fabric is continuous". Such crenulation cleavage is called 'gradational' in the terminology of Borradaile *et al.* (1982, p. 5): "gradational crenulations are laminar domains, coincident with fold limbs, the zones having diffuse, gradational boundaries through which the pre-existing fabric is continuous". 'Zonal' is *not* used here in the sense of Borradaile *et al.* (1982, p. 6) "Cleavage that occupies a considerable fraction of the rock volume. ... [we] use *zonal* only as a width descriptor".

Crenulation cleavage is not observed in the silty marl lithologies (Z91-2B and Z91-4).

In the marly slates at Wanneler Bach (Z91-8 and Z91-9) the incipient discrete and zonal crenulation cleavages appear to be slightly less developed than in similar lithologies at Linthal, which may also be reflected in the smaller c/b ratios, as they are not particularly well laminated.

Most of these crenulated slates are rich in chlorite–mica 'stacks'. A large proportion of these 'stacks', particularly the coarser ones, consist almost entirely of chlorite with very subordinate muscovite lamellae; others have mainly chloritic centres, with muscovite along the margins. The stacks in some of the more silty rocks show a marked 'expansion' (c/b aspect ratios of 1–1.5 are very common); most of these stacks consist almost entirely of chlorite. This predominance of chlorite suggests formation at the expense of clastic biotite, in addition to deposition of chlorite in the voids of extended clastic mica.

In the calcareous micaceous-silty shale beds of one bedded sample from Linthal (Z91-3) the crenulation cleavage is observed to constitute a second cleavage formed by crenulation of an earlier slaty cleavage S_1 at an angle of some 15° to the bedding; this S_1 cleavage is particularly distinct where it is marked by opaques, close to the contact with the calcareous mudstone–siltstone. This slaty S_1 fabric is the same as the crenulated bedding-parallel fabric in the other samples of this area. In the calcareous mudstone–siltstone the S_1 cleavage is absent; the S_2 cleavage domains are locally concentrated in sharp 'cleavage bundles' spaced some 1 mm apart. The high c/b in this sample is due to the absence of distinct b directions, and presence of these cleavage 'bundles'.

The cleavage of the samples from Äsch and the Friterental (north of Rübi) is not a crenulation cleavage. The cleavage domains in the calcareous silty shales (Z91-6, Z91-10 and Z91-11) are anastomosing but still continuous, and closely spaced; the microlithons are rich in bedding-parallel clastic micas and 'stacks' (Z91-6 and Z91-11). In the finer-grained shale and calcareous-shale lithology (Z91-6, 7, 11), the cleavage domains are even more closely spaced, and b-oriented clastics and stacks are very subordinate or virtually absent; the c/b in these and in other slates with very few b-oriented clastic micas is high.

Table 1. Lithology, cleavage type and location of samples

Sample No.	Lithology	Cleavage type	Locality (geological and tectonic unit in footnotes)	Swiss grid reference
Z91-1	Silty clyst.	Discrete and locally zonal crenulation. CDS 30–100 μm	1.5 km SSE of Linthal (GL), northern end of second road tunnel[1]	717.7/196.5
Z91-2A	Slate	Zonal crenulation. CDS 30–100 μm		717.7/196.5
Z91-2B	Silty carbonate; subord. calcar. silty clyst. laminae $\rightarrow$ 1.5 mm	Discrete and local zonal crenulation in clyst. laminae CDS 30–100 μm		717.7/196.5
Z91-3	Calcar. sltst.; subord. graded calcar. mdst. to silty clyst. beds $\rightarrow$ 3 mm	Discrete and some zonal crenulation in mdst. beds, CDS 50–100 μm; the crenulated S_1 is at an angle of 15–35° to the bedding		717.7/196.5
Z91-4	Silty carbonate; laminae of shale and clyst. $\rightarrow$ 1.5 mm	Local zonal crenulation in shaly laminae. CDS 50–100 μm	Chlus ('Flyschfenster'), Urnerboden Valley	709.5/191.1
Z91-5B	Quartz-rich sandy mdst.	Anastomosing discontinuous cleavage domains, exc. in cleavage "bundle"	600 m NNW of Heidmann egg ('Seelitalgraben'), Vorder Schächental[2]	703.3/192.7
Z91-6	Calcareous silty clyst.; laminae of mdst. to sltst. $\rightarrow$ 2 mm	Domainal sinuous-anastomosing (no crenulation) in clyst. CDS 20 μm (silty clyst.)–50 μm (mdst.). Discontinuous-anastomosing and "bundles" in mdst. to siltst.	NE of Äsch, Vorder Schächental[3]	705.4/191.5
Z91-7	Clayey slate	Domainal sinuous (no crenulation). CDS $\approx$15 μm		705.5/191.5
Z91-8	Slaty marl	Discrete and some zonal crenulation. Chlorite-rich domains. CDS 50–100 μm	Wanneler Bach, Vorder Schächental[3]	703.2/191.1
Z91-9	Mdst.; subord. laminae of calcar. sltst. $\rightarrow$ 0.5 mm	Discrete and some zonal crenulation in mdst. Chlorite-rich domains. CDS 40–150 μm.		703.1/191.1
Z91-10	Calcareous shale	'Reticulate' to discrete crenulation. CDS $\approx$30 μm	Fritertal, north of Friteren, Vorder Schächental[3]	702.3/192.3
Z91-11	Calcareous shale and silty carbonate	Domainal sinuous anastomosing (no crenulation). CDS $\approx$15–20 μm (shale); 50 μm (silty carbonate)		702.3/192.3
Z91-12A	Calcar. sltst.; subord. graded silty	Very fuzzy local cleavage domains	Gasperini quarry, southwest of Attinghausen (Seedorf), Reuss Valley[4]	$\approx$689.3/192.2
Z91-12B	Graded micac. clyst. to mdst.; subord. calcar. sltst. laminae $\rightarrow$ 2 mm	Fuzzy cleavage domains in mdst. laminae CDS 20–40 μm		$\approx$689.3/192.2
Z91-12C	Micac. sltst.; silty clyst. to mdst. laminae. Fold hinge	Crenulation cleavage in hinge. CDS 50–100 μm in mdst.; 20 μm in clyst.		$\approx$689.3/192.2
Z91-13	Marly mudstone	Domainal anastomosing (no crenulation). CDS 30–50 μm	*ca* 800 m southeast of Trübsee (NW), S of Engelberg[5]	$\approx$673.6/182.2
Z91-15	Micaceous slate	Anastomosing incipient cleavage	Bunderbach, east of Kandergrund, Kandertal[6]	618.3/155.4
Z91-18	Slate	'Penetrative'	West of Kandergrund, Kandertal[6]	616.3/155.6
Z91-19	Silty micaceous marl	Discontin. cleavage domains around clasts	La Tièche, ENE of Petit Mont Bonvin (VS)[7]	607.3/133.6
Z91-20	Very fine muddy sandst.	No distinct cleavage		607.3/133.7

Z91-21	Microfolded calcar. silty clyst. or slaty marl	Domainal sinuous-anastomosing (no crenulation). CDS 20–40 μm	300 m south of Lac de Derborence (VS)[8]	582.9/124.9
Z91-22	Laminated mdst. and calcar. sandy mdst.	No distinct cleavage	*ca* 700 m southeast of Solalex, Anzeinde Valley (VD)[9]	577.2/125.9
Z91-23	Calcar. sandst.; subord. graded micac. mdst.	No cleavage		577.2/125.9
Z91-25	Laminated calcar. silty clyst. and mdst.	Domainal discontinuous anastomosing (no crenulation). CDS ≈30 μm	*ca* 0.5 km northeast of Taveyanne, Haute	576.1/128.3
Z91-26	Marly clyst. and silty micac. laminae	Domainal sinuous anastomosing (no crenulation). CDS ≈20 μm	Gryonne Valley (VD)[8]	576.1/128.3
Z91-29A	Marl and silty marl	Anastomosing incip. cleavage. CDS 20–50 μm	Creux de Culan, south of Les Diablerets Village (VD)[9]	577.9/129.5
Z91-29B	Silty marl	Anastomosing incip. cleavage. CDS 20–50 μm		577.9/129.5
Z91-31	Calcareous slate	Marked penetrative. CDS ≤ 20 μm	Bunderbach, east of Kandergrund, Kandertal[6]	618.3/155.4
Z91-32A	Graded calcar. silty micac. mdst. to clyst.; calcar. sltst. laminae	Weak domainal discontinuous anastomosing (no crenulation); marked in 1 mm clyst. adjac. to sltst. CDS 20–40 μm	Gasperini quarry, southwest of Attinghausen, Reuss (Seedorf) Valley[3]	≈689.5/192.2
Z91-32B	Graded calcar. micac. mdst. to clyst. and laminated calcar. sltst.	Weak discontinuous anastomosing cleavage domains in mdst.; marked in 1 mm adjacent to sltst. CDS ≈30–50 μm.		≈689.5/192.2

Abbreviations: sltst., siltstone; mdst., mudstone; clyst., claystone; CDS, cleavage domain spacing; calcar., calcareous; micac., micaceous; subord, subordinate.
Note: samples with A, B, etc., suffixes were collected from the same localities.
[1]Transition of Taveyannaz-Series to the overlying 'Flysch sandstones' (=so-called 'Altdorfer Sandstones' auctorum)' (F. Frey in Brückner *et al.*, 1967, p. 665).
[2]Lowermost Liassic near base of Axen nappe (M. Frey in Frey *et al.*, 1980, pp. 299-300).
[3]'Taveyannaz sandstone (with shale beds)' in North-Helvetic Tertiary ('North-Helvetic Flysch') (Brückner and Zbinden, 1980).
[4]'Lower Altdorf Sandstone (Sandstone of Elm, Attinghausen, etc.)' in North-Helvetic Tertiary ('North-Helvetic Flysch') (Brückner and Zbinden, 1980).
[5]Parautochthonous and autochthonous Tertiary.
[6]Probable Diablerets Flysch.
[7]Jägerchrüz wedge, overlying the parautochthonous Doldernhorn nappe (Bugnon, 1981).
[8]Plaine-Morte flysch (Ultrahelvetic) (cf. Badoux and Gabus, 1990).
[9]Morcles flysch (cf. Badoux and Gabus, 1990).

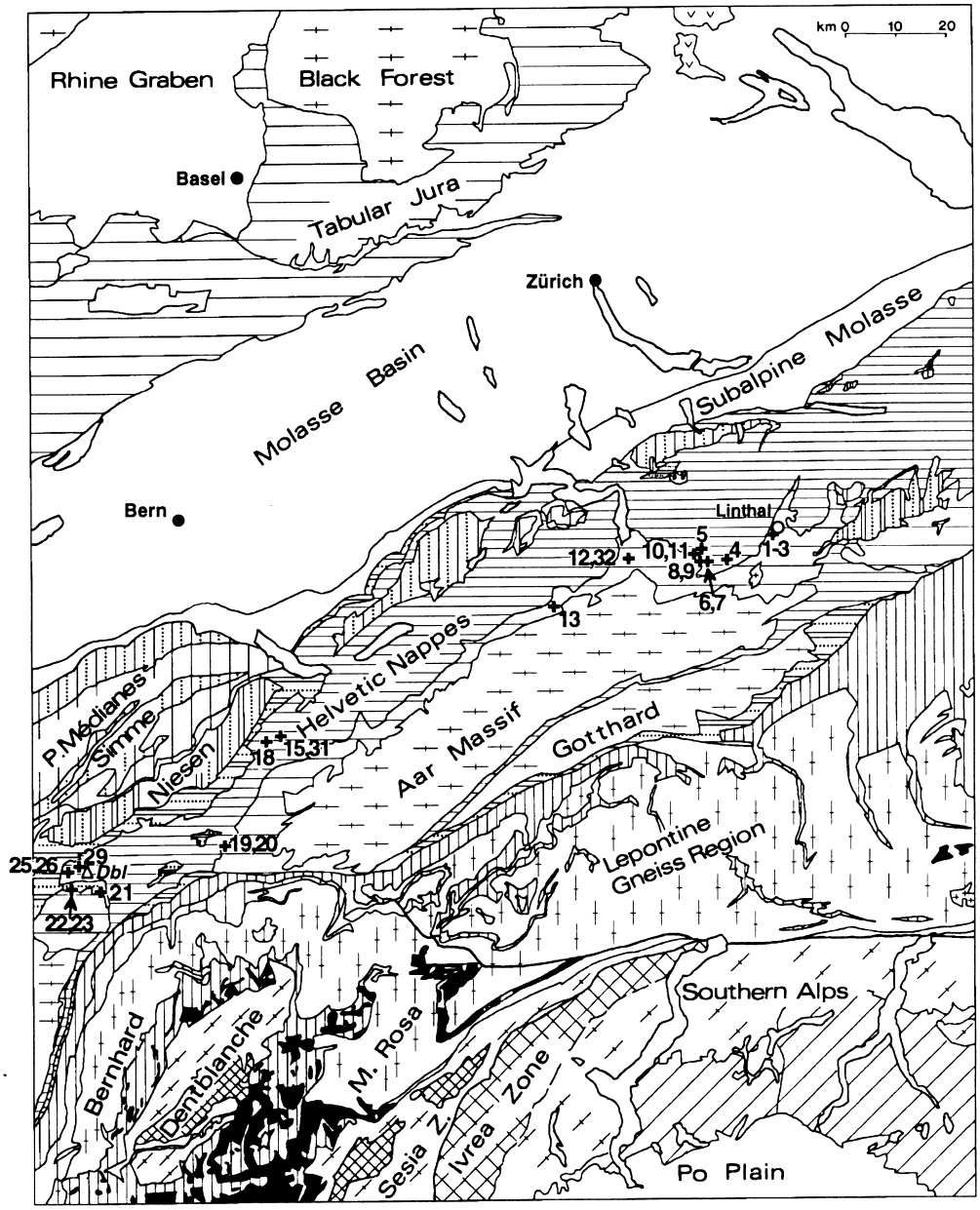

Fig. 1. Simplified tectonic map of the central Alps showing localities of the samples discussed. Modified from Laubscher and Bernoulli (1980, fig. 1—based on Spicher, 1980). The horizontal line ornament indicates the Mesozoic and Tertiary of the foreland and cover of external massifs, and of the Helvetic and Ultrahelvetic nappes; the vertical lines denote the Pennine nappes. Abbreviations: Dbl, Les Diablerets mountain.

(2) Gasperini quarry near Attinghausen–Seedorf (Reuss Valley)

Samples from this locality show a pronounced lithological bedding lamination on a scale of 1–4 mm, with alternation of beds of calcareous micaceous mudstone with calcite-cemented micaceous siltstone–fine sandstone.

Cleavage is visible only in the mudstone beds. The cleavage domains are very discontinuous–anastomosing and consist mainly of opaques (?rutile) or are fuzzy. In the fold hinges (Z91-12C) there is a local crenulation cleavage marked by opaque seams, with poor continuity and without mica reorientation.

The samples from this locality appear to differ from those of the previous area only in having a much weaker crenulation cleavage superimposed on the marked lamination and strong bedding-parallel fabric.

(3) Kandertal, La Tièche and Diablerets area

No distinct crenulation cleavages were found in the samples collected. They cover a wide range of textures, ranging from only very incipient cleavage domains

(Z91-15, Kandergrund), through irregular, discontinuous 'wiggly' opaque cleavage domains (Z91-19, La Tièche), and sharp, closely-spaced cleavage domains, either mainly marked by opaques and with many stacks (Z91-21, Derborence), or more micaceous with some clastic bedding-parallel mica but few stacks (Z91-25 and 26, Taveyanne), to a virtually penetrative cleavage without cleavage domains or clastic micas at a large angle to the cleavage domains (Z91-18, Kandergrund; Z91-31, Kandergrund).

The cleavage domains in some of these samples are mica-poor and are predominantly marked by opaques. The fine-grained phyllosilicates in the microlithons appear to be largely oriented in the cleavage direction (although this is often difficult to assess due to the high carbonate content of the microlithons).

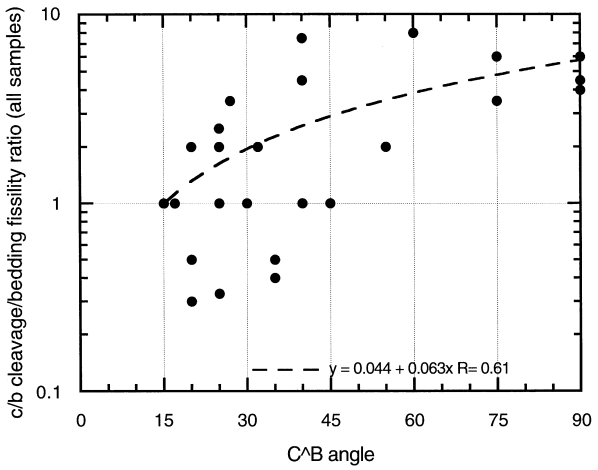

Fig. 2. Variation of the c/b cleavage/bedding fissility ratio with the C^B angles. The high c/b cleavage/bedding fissility ratios are associated with large C^B angles.

METHODS

Aspect ratios of fissility fragments

The cleavage/bedding fissility ratios after Durney and Kisch (1994), (the c/b fissility ratio or c/b ratio), were measured in the field. The measurements of the aspect ratios of the fissility fragments were made on the actual cleavage and bedding directions, even where these are not perpendicular, rather than orthogonal, for instance in the c and ^c directions, and then angle-corrected to oblique c/b values.

When evaluating the c/b fissility ratios, it should be realized that the bedding and cleavage of some of the samples measured in the field and collected were far from being at a moderate to high angle, as required by Durney and Kisch (1994, p. 270): the $C \leq B$ angles diverged widely, in some cases being as small as 20°. In order to assess to what extent the value of the c/b fissility ratio might be affected by the small $C \leq B$ angles, they were plotted against each other (Fig. 2). The plot shows a distinct tendency for low c/b fissility ratios (<1) to be associated with small $C \leq B$ angles, and for the samples with the large $C < B$ angles to yield high c/b fissility ratios.

Illite 'crystallinity'

The current awareness of the effect of slide thickness on the measured 10 Å half-height peak widths (Kisch, 1991; Frey, 1988; Krumm and Buggisch, 1991) did not exist at the time of the earlier illite 'crystallinity' measurements (Kisch, 1980): many of the slides prepared at the time were probably too thin, and the peak widths measured consequently somewhat too narrow, yielding anomalously high degrees of metamorphism. For this reason, new illite 'crystallinity' (IC) measurements were measured on appropriately thick slides of the $<2\,\mu$m fractions of the samples collected for this study; these new values are given in Table 2. The scale used is the one earlier adopted by Kisch, in which the high- and low-grade limits of the anchizone correspond to 10 Å peak half-height widths of, respectively, 0.19° and 0.37°$\Delta 2\Theta$ (in the $<2\,\mu$m size fraction).

X-ray diffraction intensity ratios of phyllosilicate 00 l reflections

The methods of measurement are those developed in the paper by Kisch (1994), to which the reader is referred for further details. The slabs were cut parallel to the cleavage and bedding directions determined in the field; with five exceptions (and those only for the bedding-parallel slabs), they were cut at a width of at least 18 mm. The intensities of the low-angle basal mica and chlorite reflections at 10 Å and 7 Å used for the calculation of the intensity ratios were measured using a divergence/scatter slit set of 0.5°; in addition, these intensities were measured using a divergence/scatter slit set of 1° (see below). Higher-angle reflections were measured using a divergence/scatter slit set of 1° only. All reflections—using either slit set—were measured without removing the slab from the sample holder.

Tests of reproducibility using 1° and 0.5° slit sets. The earlier paper (Kisch, 1994, pp. 257–258) advocated the use of the intensity ratios of the same reflection as measured using 1° and 0.5° slit sets—specifically that at 10 Å, i.e. the $I_{10Å\ (0.5°)}/I_{10Å\ (1°)}$ intensity ratio—to monitor mispositioning of the slab in the goniometer: this ratio is then reduced, as the decrease in intensity of the reflection upon mispositioning in the goniometer as measured with the 0.5° slit—when a correctly positioned 20 mm sample at a diffraction angle of 8.95°$\Delta 2\Theta$ (10 Å) almost completely intersects the X-ray beam—is much stronger than as measured with the 1° slit set, when the X-ray beam is much wider than the slab. In the current study both the $I_{10Å\ (0.5°)}$/

Table 2. Data for the studied samples: cleavage/bedding fissility ratios, widths and phyllosilicate peak intensities of C- and B-parallel slabs, peak-intensity ratios $I_{10Å\ (0.5°)}$ C/B and $I_{10Å}/I_{7Å}$ C/B, and mica–illite 'crystallinities' measured on the slabs and two size fractions

Sample No., Locality	*c*/*b* fissility ratio	C slab			B-slab			$I_{10Å}$ C/B	$I_{10Å}/I_{7A°}$ C/B	C ∧ B	$(1 - I_{29.5°}* - I_{20.8°}*)$ C/B	$I_{10Å}$ C/B*	IC slabs mean width (°Δ2Θ)	IC powder size fractions	
		Width	$I_{10Å}$ C	$I_{7Å}$ C	Width	$I_{10Å}$ B	$I_{7Å}$ B							< 2 μm	2–6 μm
Z91-1 Linthal	2.0*	26.0	1820	2300	15.0	630	2240	2.889	2.813	32	1.4	2.0	0.189	0.287	0.250
Z91-2A Linthal	1.0*	27.0	562	902	19.5	1151	2050	0.488	1.110	25	1.1	0.43	0.199	0.270	0.230
Z91-2B Linthal	2.0*	25.0	696	1056	28.0	300	912	2.320	2.004	25	1.4	1.7	0.187	0.283	0.280
Z91-2B Linthal re-run1–2 (12/93)	2.0*	25.0	888	1232	26.0	304	1076	2.684	2.525	25			0.191	0.283	0.280
Z91-3 Linthal (11/93)	3.5†	28.0	84	276	26.0	268	1188	0.313	1.349	75			0.198	0.295	0.250
Z91-4 Chlus	1.0*	24.0	94	262	26.0	724	1256	0.130	0.622	45	0.92	0.14	0.198	0.300	0.303
Z91-5B Seelital	2.0	28.0	92	550	27.0	180	532	0.511	0.494	55	1.1	0.49			
Z91-6 ENE Äsch (11/93)	3.5	29.0	136	324	26.0	188	492	0.723	1.099	27	1.0	0.71	0.263	0.330	0.325
Z91-7 ENE Äsch	6.0	26.0	660	1208	12.0	60	168	11.00	1.530	75	0.80	14	0.320	0.425	
Z91-8 Wanneler Bach	0.33*	26.0	352	950	18.0	800	2040	0.440	0.945	25	1.0	0.43	0.205	0.300	0.268
Z91-9 Wanneler Bach	0.50*	24.0	352	1084	26.0	836	2310	0.421	0.897	20	1.1	0.40	0.192	0.285	
Z91-10 Friteren (11/93)		28.5	356	720	27.0	188	388	1.894	1.020	22	1.0	1.8	0.288	0.355	0.320
Z91-11 Friteren	7.5	24.0	449	641	13.0	140	774	3.207	3.873	40	0.97	3.3	0.239	0.327	0.287
Z91-11 Friteren re-run (11/93)	7.5	27.5	552	784	19.0	182	932	3.033	3.606	40			0.243	0.327	0.287
Z91-12A Attinghausen (Seedorf) C wide (11/93)	0.50	26.0	148	110	28.5	1480	720	0.100	0.654	20	1.2	0.087	0.155	0.507	0.300
Z91-12A Attinghausen (Seedorf) C narrow (11/93)	0.50	23.0	218	168						20				0.507	0.300
Z91-12B Attinghausen (Seedorf)	0.40	25.0	296	204	22.0	1480	590	0.200	0.578	35	0.95	0.21	0.157	0.472	0.278
Z91-12C Attinghausen (Seedorf)	1.0	29.0	791	538	21.0	166	102	4.765	0.903	30	1.6	2.9	0.213	0.415	0.240
Z91-12C Attinghausen (Seedorf) re-run (12/93)	1.0	28.0	804	536	21.0	156	122	5.154	1.173	30			0.220	0.415	0.240
Z91-13 Trübsee	2.5	28.0	800	1940	27.0	116	372	6.897	1.322	25	1.2	5.9	0.245	0.260	0.223
Z91-15 Bunderbach (11/93)	0.33	27.0	276	408	27.0	1148	1372	0.240	0.808	25	0.92	0.26	0.200	0.470	0.387
Z91-18 Kandergrund-W	1.0	24.0	1200	816	22.0	616	480	1.948	1.146	17	1.0	1.9	0.262	0.545	0.333
Z91-19 La Tièche	2.0	22.0	272	470	22.0	376	588	0.723	0.905	20	0.88	0.82	0.211	0.425	0.270
Z91-20 La Tièche	1.0	25.0	58	100	26.0	68	164	0.853	1.399	40	1.0	0.84	0.201	0.375	0.235
Z91-21 Derborence	6.0	26.0	644	712	28.0	96	356	6.708	3.354	90		6.7	0.337	0.352	0.287
Z91-22 Solalex (14/10)	1.0	25.0	116	172	23.0	112	126	1.036	0.759		0.80	1.3		0.390	0.330
Z91-22 Solalex (25/10)	1.0	25.0	124	180	23.0	140	144	0.886	0.698		0.88	1.0	0.251	0.390	0.330
Z91-23 Solalex	0.50	28.0	36	24	25.0	104	316	0.346	4.558	35	0.66	0.53	0.251	0.600	0.360
Z91-25 Taveyanne	4.0	24.0	112	260	17.0	72	172	1.556	1.029	90	1.1	1.4	0.220	0.450	0.290
Z91-26 Taveyanne	2.0	27.0	415	670	24.0	400	764	1.038	1.183	25	1.1	0.91	0.224	0.442	0.275
Z91-29A Creux de Culan	4.5	24.0	248	432	26.0		88			40	3.0			0.742	0.343
Z91-29B Creux de Culan	4.5	27.0		80	27.0	48	112			90	0.75			0.790	0.340
Z91-31 Bunderbach	8.0	25.0	404	480	15.0	40	96	10.10	2.020	60	0.96	10		0.420	0.275
Z91-32A Attinghausen (Seedorf)	0.30	27.0	714	376	26.0	608	284	1.174	0.887	20	0.97	1.2	0.240	0.363	0.277
Z91-32B Attinghausen (Seedorf)	1.0	26.0	538	364	23.0	584	388	0.921	0.982	15	1.1	0.85	0.234	0.360	0.270

*In the samples with an S_2 crenulation cleavage, *c* refers to this crenulation cleavage, and *b* is a combination of the bedding and the earlier bedding-parallel S_1 cleavage;
†In sample Z91-3, in which the earlier cleavage S_1 is at an angle to the bedding, *b* refers to the bedding as *distinct* from the S_1 slaty cleavage.

$I_{10Å\ (1°)}$ and $I_{7Å\ (0.5°)}/I_{7Å\ (1°)}$ intensity ratios were used for this purpose (Fig. 3). The usual ranges of these intensity ratios are, respectively, 0.35–0.75 and 0.30–0.70; measurements on four slabs for which these ratios fell outside these ranges were rejected. However, in this case mispositioning is unlikely to be the main reason for the anomalous ratios, as the slabs were not removed from the goniometer upon changing the slit set and care was taken to position them correctly. Inspection of these slabs and the peak height measured shows that these anomalous ratios can confidently be attributed to two other factors.

1. Lithological inhomogeneity in the slab. In three of these slabs a cm-scale swath of different composition extends along the long slab axis which is inserted parallel to the goniometer axis (and thus also to the slit length). At the low diffraction angles of 8.85°2Θ (10 Å) and 12.6°2Θ (7 Å), the 1° beam is wider than the widest slabs used: the 1° slit set will thus illuminate the whole slab width and integrate its lithology, whereas the 0.5° slit set will preferentially illuminate the central strip, and highlight its divergent lithology. The result is an anomalous ratio of the intensities of the same reflection as measured with 1° and 0.5° slits.
2. Very low peak heights. The very weak 10 Å reflections (<40 c.p.s.) measured on a few slabs using the 0.5° slit set cannot be measured with any degree of accuracy; these result in very imprecise $I_{10Å\ (0.5°)}/I_{10Å\ (1°)}$ intensity ratios for these slabs.

Correction for lithological heterogeneity. The $I_{10Å\ (0.5°)}$ C/B ratio strictly reflects the mica fabric only when the C and B slabs sample the same microfabric, i.e. lithology and mica content. However, because of the ubiquitous presence of some bedding inhomogeneity in layered metasedimentary rocks, the C slab unavoidably tends to represent a somewhat more varied lithology and concomitant phyllosilicate content than does the B slab. The difference in lithology between the C and B slabs of some samples is evident from the difference in the content of quartz and calcite, the major non-phyllosilicate phases present. In order for the $I_{10Å\ (0.5°)}$ C/B ratio to represent the phyllosilicate fabric rather than the difference in lithology/phyllosilicate content between the C and B slabs, the intensities of the phyllosilicate reflections in both slabs need to be normalized to the same phyllosilicate content.

In an earlier paper (Kisch, 1994, p. 259), it was proposed to normalize the absolute intensities of the phyllosilicate reflections to those in quartz-free samples using the intensity of a quartz reflection. In this study, this was done for both quartz and calcite, the total phyllosilicate content of the slabs being approximated by subtracting the calcite + quartz content from the total. The quartz and calcite contents were assessed from the intensities of their diffraction peaks at, respectively, 20.85° 2Θ (4.255 Å) and 29.5° 2Θ (3.028 Å—10–14). In order to use these peak intensities as parameters of mineral content in the C and B slabs, it has to be ascertained that they are not affected by orientation effects. A plot of the ratios of the intensities of the reflections in the C and the B slab of the same sample against the $I_{10Å\ (0.5°)}$ C/B ratio showed no such effects. Because the 10–14 peak of calcite (primitive rhombohedral cell) corresponds to the cleavage rhombohedron *r* ({10–11} or {100} in the face-centred rhombohedral cell) whose faces are at angles of 44°36.5′ with (0001) and of 75°55′ to each other, no enhancement upon reorientation is to be expected. The content of each of these minerals is therefore taken as the intensity of the diffraction peak ($I_{peak\ slab}$) normalized to its intensity in a slab of the pure mineral ($I_{peak\ pure\ mineral}$), i.e. $I_{peak\ slab}/I_{peak\ pure\ mineral}$, hence I_{peak}*. The total phyllosilicate content in the slab is then approximated by

$$1 - I^*_{29.5°\ calcite} - I^*_{20.8°\ quartz},$$

and the normalized $I_{10Å\ (0.5°)}$ C/B ratio, $I_{10Å\ (0.5°)}$ C/B*, is obtained by dividing the measured $I_{10Å\ (0.5°)}$ C/B ratio by the ratio of the approximate phyllosilicate contents in the C and B slabs, i.e.

$$(1 - I^*_{29.5°\ calcite} - I^*_{20.8°\ quartz})C\ slab \div (1 - I^*_{29.5°\ calcite} - I^*_{20.8°\ quartz})\ B\ slab.$$

The correctness of this procedure was tested by plotting the $I_{10Å\ (0.5°)}/I_{4.46Å\text{-}19.9°\ (1°)}$ C/B against both the measured $I_{10Å\ (0.5°)}$ C/B ratio and the corrected $I_{10Å\ (0.5°)}$ C/B* ratio; a markedly better fit is obtained

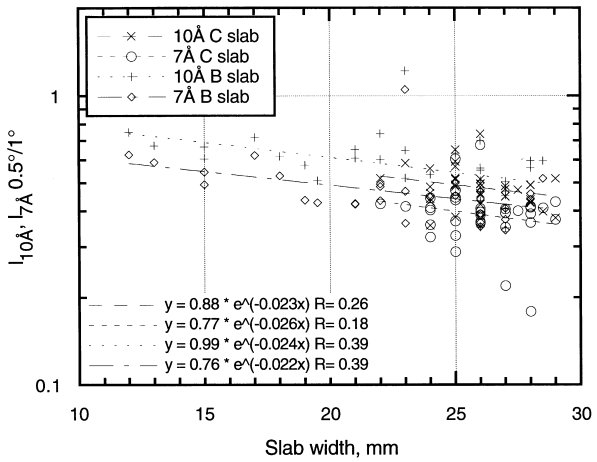

Fig. 3. Ratio of peak intensities of two low-angle reflections as measured on the slabs with 1° and 0.5° slit sets. Note that the intensity ratios are consistently lower for the lower-angle illite 10 Å (8.8°2Θ) than for the higher-angle chlorite 7 Å (12.5°2Θ) reflections. Strongly divergent ratios ($I_{0.5°\ slits}/I_{1°\ slits} > 0.75$ or < 0.30) are due either to very low measured intensities of the $I_{10Å\ (0.5°)}$ reflections (less than 40 c.p.s.), or to probable measurement errors (in this case the intensity ratios $I_{0.5°\ slits}/I_{1°\ slits}$ are anomalous for both the illite 10 Å (8.8°2Θ) and the chlorite 7 Å (12.5°2Θ) reflections as measured on the same slab).

in the latter ($R = 0.972$) than in the former ($R = 0.889$) case. This procedure might be further perfected by also correcting for differences in the content of further minor non-phyllosilicate phases present, such as albite and dolomite, but this has not been done in the present study.

RESULTS

Metamorphic grade—illite 'crystallinity'

The results of the new illite 'crystallinity' (IC) measurements on appropriately thick slides of the $< 2\ \mu$m fractions of the samples collected for this study are given in Table 2.

1. Linthal, Urnerboden and upper Schächental. The peak-width values range between 0.27 and 0.30°$\Delta 2\Theta$, with somewhat broader, low-anchizonal to 'diagenetic' values (0.33–0.42°$\Delta 2\Theta$) at Äsch and Friteren.
2. Gasperini quarry near Attinghausen–Seedorf (Reuss Valley). IC values of 0.35–0.55°$\Delta 2\Theta$ were measured earlier (Kisch, 1980, Table 1); re-measurement gave a similar range of 0.36–0.51°$\Delta 2\Theta$.
3. Kandertal, La Tièche, and Diablerets areas. The samples have 'diagenetic' illite 'crystallinity' values ranging from *ca* 0.40°$\Delta 2\Theta$ (La Tièche), *ca* 0.45°$\Delta 2\Theta$ (Taveyanne), through 0.47–0.54°$\Delta 2\Theta$ (Kandergrund, Taveyanne) to 0.74–0.79°$\Delta 2\Theta$ (Creux de Culan, Diablerets); only the sample from Derborence has a higher-grade, low-anchimetamorphic illite 'crystallinity' of 0.35°$\Delta 2\Theta$.

Phyllosilicate orientation and cleavage/bedding fissility ratio

The c/b fissility ratios as measured in the field and the $I_{10\text{Å}\ (0.5^\circ)}$ C/B* intensity ratios are listed in Table 2. The values range, respectively, from 0.3 to 8, and from 0.01 to 14.

The c/b fissility ratio has been plotted against the $I_{10\text{Å}\ (0.5^\circ)}$ C/B* intensity ratio for all the samples investigated (Fig. 4). This plot shows considerable scatter, with a power regression

$$c/b = 1.28 \times (I_{10\text{Å}\,(0.5^\circ)}\text{C/B}^*)^{0.589}\ (R = 0.789).$$

The sense of divergence of the sample points from this regression shows a relationship to the lithology: particularly low c/b values for given $I_{10\text{Å}\ (0.5^\circ)}$ C/B* intensity ratios are shown by the siltstones and very fine sandstones, and by all the samples from the Gasperini quarry, most of which contain subordinate to predominant siltstone and very-fine sandstone beds, and a marked lithological bedding inhomogeneity. When

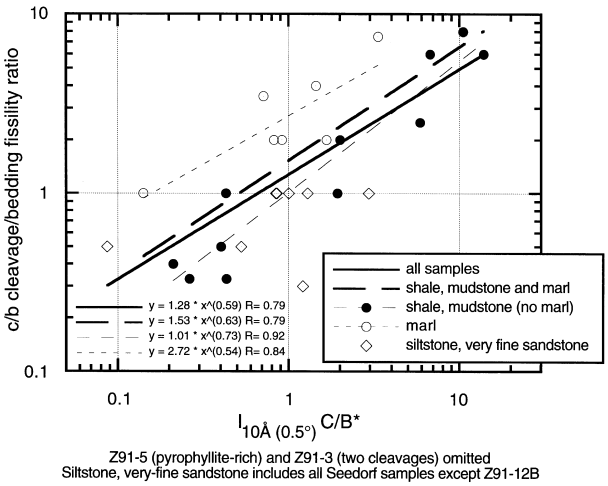

Fig. 4. Variation of the c/b cleavage/bedding fissility ratios with the $I_{10\text{Å}\ (0.5^\circ)}$ C/B* intensity ratios: relation to lithology. Regressions are given for (1) all samples; (2) shale, mudstone and marl (i.e. all samples excluding siltstone and very fine sandstone); (3) calcite-poor shale and mudstone (full dots); and (4) marl (open dots).

these siltstones and very fine sandstones are not taken into consideration (Fig. 4), a power regression

$$c/b = 1.53 \times (I_{10\text{Å}\,(0.5^\circ)}\text{C/B}^*)^{0.589}\ (R = 0.794)$$

is obtained, which is rather similar to the regression

$$c/b = 1.45 \times (I_{10\text{Å}\,(0.5^\circ)}\text{C/B})^{0.462}\ (R = 0.557)$$

found earlier for a series of mudstone samples from the Caledonides of the Mörsil-Järpen area in Jämtland, western central Sweden (Kisch, 1994).

In contrast, the marly samples show relatively high c/b fissility ratios (defined as marls here are all non-siltstone–sandstone samples with $I_{\text{calcite}\ 29.5^\circ}$ (average C, B) > 2800 cps). When the shale–mudstone and marly and siltstone–very fine sandstone lithologies are plotted separately (Fig. 4), two close to parallel power regression lines are obtained for the mudstone and marly samples, the marly lithologies showing much higher c/b cleavage bedding fissility ratios for a given $I_{10\text{Å}\ (0.5^\circ)}$ C/B* intensity ratio ($c/b = 2.72 \times (I_{10\text{Å}\ (0.5^\circ)}$ C/B*$)^{0.542}$ ($R = 0.829$)) than the shale–mudstones ($c/b = 1.01 \times (I_{10\text{Å}\ (0.5^\circ)}$ C/B*$)^{0.735}$ ($R = 0.924$)); the siltstone–very fine sandstones show the lowest c/b fissility ratios for a given $I_{10\text{Å}\ (0.5^\circ)}$ C/B* intensity ratio, and a smaller increase in the c/b cleavage bedding fissility ratios with the $I_{10\text{Å}\ (0.5^\circ)}$ C/B* intensity ratio than the other lithologies.

Another conceivable effect on the relationship between the c/b fissility ratio and the $I_{10\text{Å}\ (0.5^\circ)}$ C/B* intensity ratio is the grade of metamorphism as expressed by the illite 'crystallinity' values in the $< 2\ \mu$m fraction. For instance, enhanced recrystallization of phyllosilicates in the cleavage direction at higher metamorphic grades, particularly in the microlithons, would conceivably affect the $I_{10\text{Å}\ (0.5^\circ)}$ C/B* intensity ratio more than the c/b fissility ratio. In order

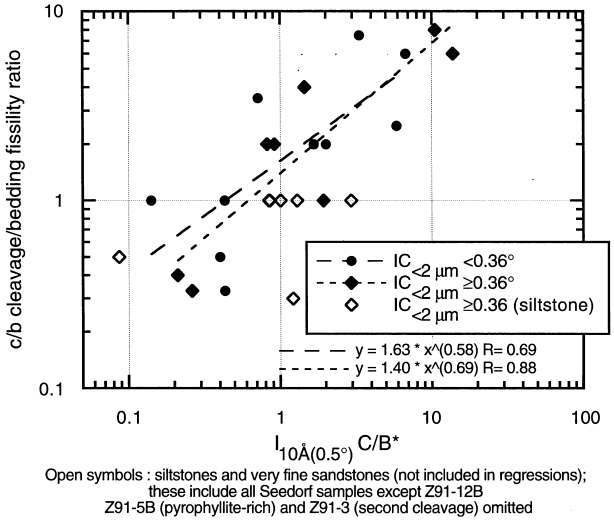

Fig. 5. Variation of the c/b cleavage/bedding fissility ratios with the $I_{10Å\ (0.5°)}$ C/B* intensity ratios: relation to illite 'crystallinity' ($<2\ \mu m$ size fraction). Separate regressions are given for shale, mudstone and marl samples with $IC_{<2\ \mu m} < 0.36°\Delta 2\Theta$ and $IC_{<2\ \mu m} \geq 0.36°\Delta 2\Theta$. No regression given for the siltstone and very fine sandstone (all with $IC_{<2\ \mu m} \geq 0.36°\Delta 2\Theta$).

to assess this effect the points were divided into two classes of illite 'crystallinity' values, $IC_{<2\ \mu m} < 0.36°\Delta 2\Theta$ and $IC_{<2\ \mu m} \geq 0.36°\Delta 2\Theta$; the first group includes all except one of the samples from Linthal, Urnerboden and the Schächental. However, the plot of the c/b fissility ratio against the $I_{10Å\ (0.5°)}$ C/B* intensity ratio showing these two classes of illite-'crystallinity' values (Fig. 5) shows that the effect of the degree of metamorphism is only very minor, expressed mainly at the lower $I_{10Å\ (0.5°)}$ C/B* intensity ratios.

A major difference appears to be the presence of the initial crenulation cleavage common in the samples from the Urnerboden and Schächental valleys (see section on microfabrics). As shown above, this crenulation cleavage is a second cleavage crenulating an earlier slaty cleavage fabric, which is bedding-parallel in most of the samples studied but locally at a distinct angle to the bedding. The crenulated samples have lower $I_{10Å\ (0.5°)}$ C/B* intensity ratios (0.4–2 vs 0.7–13) and c/b cleavage bedding fissility ratios (0.3–2 vs 1–8) than most of the non-crenulated slates, mudstones and marls (Fig. 6); the presence of crenulation cleavage has a somewhat stronger effect on the c/b cleavage–bedding fissility ratios than on the $I_{10Å\ (0.5°)}$ C/B* intensity ratios. These reduced ratios must mean that the strong b-parallel orientation of the phyllosilicates, presumably reflecting the enhancement of the bedding-parallel fabric by the S_1 slaty-fabric in the microlithons, predominates over any c-parallel phyllosilicate orientation in the crenulation-cleavage domains. For good order, it should be noted that the small c/b fissility ratios in the crenulated samples could in part reflect the small C < B angles measured in most of these samples.

In parallel with the above is the tendency for the slates, mudstones and marls—i.e. all samples except the siltstones–very fine sandstones and the strongly bedding-laminated samples from the Gasperini quarry—with a closely spaced ($\leq 30\ \mu m$) domainal cleavage to show higher values of the c/b fissility ratio for given $I_{10Å\ (0.5°)}$ C/B* intensity ratios than the samples showing a more widely spaced (50–150 μm) domainal cleavage; the latter include those with an incipient crenulation-cleavage and phyllosilicate-rich cleavage domains (Fig. 7).

Illite/chlorite ratios in the cleavage and bedding directions

In order to assess the possible preferential formation of illite or chlorite in the cleavage relative to the bedding as cleavage formation progresses, the mica/chlorite ratio in the C slab divided by that in the B slab,

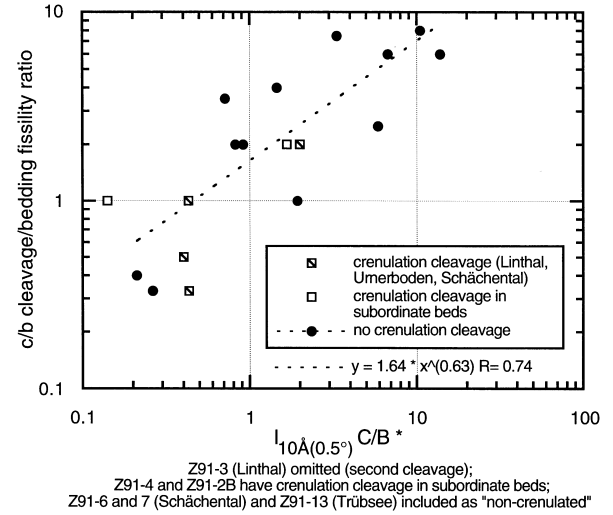

Fig. 6. Variation of the c/b cleavage/bedding fissility ratios with the $I_{10Å\ (0.5°)}$ C/B* intensity ratios: relation to presence or absence of crenulation cleavage.

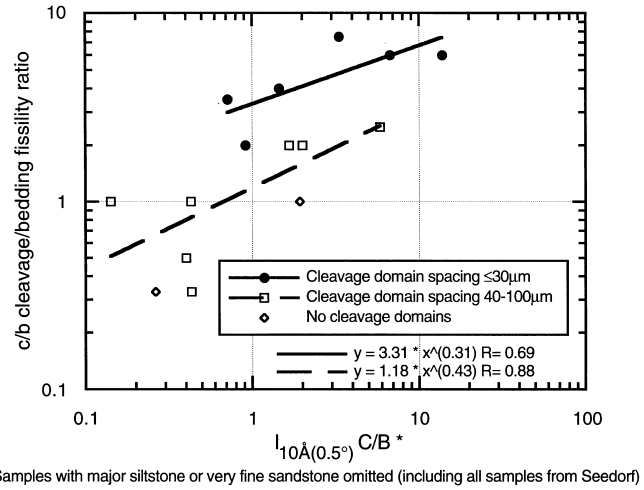

Fig. 7. Variation of the c/b cleavage/bedding fissility ratios with the $I_{10Å\ (0.5°)}$ C/B* intensity ratios: relation to the cleavage-domain spacing.

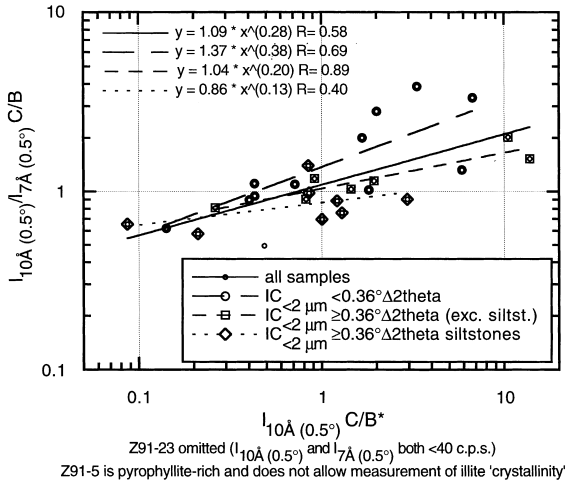

Fig. 8. Variation of the $I_{10Å\ (0.5°)}/I_{7Å\ (0.5°)}$ C/B ratios with the $I_{10Å\ (0.5°)}$ C/B* intensity ratios: relation to illite 'crystallinity' ($<2\ \mu$m size fraction). Separate regressions are given for shale, mudstone and marl samples with $IC_{<2\ \mu m} < 0.36°\Delta 2\Theta$ and $IC_{<2\ \mu m} \geq 0.36°\Delta 2\Theta$. No regression given for the siltstone and very fine sandstone (all with $IC_{<2\ \mu m} \geq 0.36°\Delta 2\Theta$).

hence referred to as the $I_{10Å}/I_{7Å}$ C/B ratio, was plotted against the $I_{10Å\ (0.5°)}$ C/B* ratio (Fig. 8).

As found by Kisch (1994), there is a distinct tendency for the illite/chlorite ratio to be somewhat lower in the C slab that in the B slab in the incipient development of phyllosilicate orientation, but to markedly increase with increasing phyllosilicate orientation, so as to be almost uniformly higher when the $I_{10Å\ (0.5°)}$ C/B* ratio exceeds unity. This increase in the $I_{10Å}/I_{7Å}$ C/B ratio is markedly stronger for the 'higher-grade' samples with $IC_{<2\ \mu m} < 0.36°\Delta 2\Theta$ than for the 'lower-grade' samples with $IC_{<2\ \mu m} \geq 0.36°\Delta 2\Theta$; these 'higher-grade' samples ratios either contain chlorite-predominant mica–chlorite stacks, or show strong reorientation of clastic mica in the cleavage.

It is rather striking that if the $I_{10Å}/I_{7Å}$ C/B ratio is plotted directly against the c/b fissility ratio, rather than against the $I_{10Å\ (0.5°)}$ C/B* ratio, a rather good positive relationship is obtained, which is even somewhat better than the relationship between the c/b fissility ratio and the $I_{10Å\ (0.5°)}$ C/B* ratio. Again, the effect is stronger for the 'higher-grade' ($IC_{<2\ \mu m} < 0.36°\Delta 2\Theta$) than for the 'lower-grade' ($IC_{<2\ \mu m} \geq 0.36°\Delta 2\Theta$) samples.

Degree of tectonic fabric development: the i/b intersection/bedding fissility ratio

Most of the i/b intersection/bedding fissility ratios measured on the Helvetide samples (Fig. 9) plot in a roughly I-constant band parallel to the c/b axis, predominantly in the high i/b ratio part of the 'Manilla mudstone field', i.e. towards the 'shale field' (Durney and Kisch, 1994, figs 12 and 15). The average initial bedding/cleavage fissility ratio b_0/c_0, obtained by projecting the samples back to the -C axis (or i/b = 1 axis) along parallel loci, is 5 (the reciprocal of the initial cleavage/bedding fissility ratio of $c_0/b_0 = 0.2$), or 'strong' according to the divisions of Durney and Kisch (1994, fig. 4). However, as for the c/b cleavage/bedding fissility, the i/b ratios for the crenulated samples from the Linthal–Urnerboden–Schächental area (from 2 to 5) are rather smaller than for most of the other samples, which may be indicative of a higher initial bedding anisotropy (b_0/c_0)—which may explain the lower c/b fissility ratios—and/or a different deformation style for these samples (see Discussion).

DISCUSSION

Microfabric and the relationship between phyllosilicate orientation and fissility morphology

Scatter in plots of the c/b fissility ratios against the $I_{10Å\ (0.5°)}$ C/B* intensity ratios reflects differences in the relative development of cleavage fissility and the total phyllosilicate fabric, i.e. in the cleavage domains *and* the microlithons: a high c/b fissility ratio for a low $I_{10Å\ (0.5°)}$ C/B* intensity ratio reflects strong cleavage fissility for little overall cleavage-parallel phyllosilicate orientation, and vice versa. Cleavage-domain development enhances the development of cleavage fissility, even in rocks showing little cleavage-parallel phyllosilicate orientation or retaining a strong bedding-parallel (or S_1-parallel) fabric in the microlithons, and therefore showing low $I_{10Å\ (0.5°)}$ C/B* intensity ratios. In the extreme case of cleavage domains consisting mainly or entirely of non-phyllosilicate minerals such as opaques, iron oxides and organic matter, without major

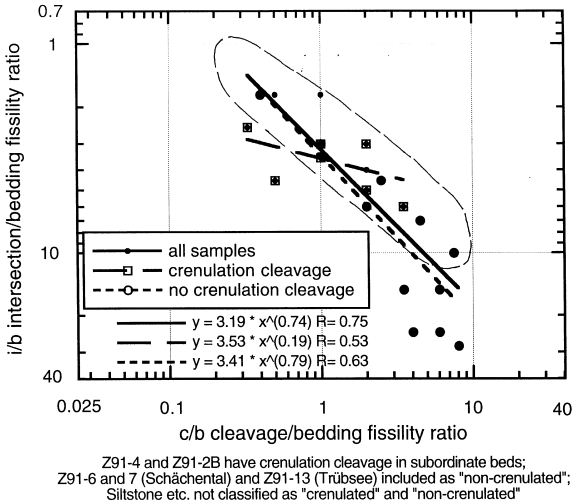

Fig. 9. Three-axis plot of three-dimensional fissility ratio measurements c/b and i/b after Durney and Kisch (1994). In departure of the plot proposed by Durney and Kisch, in which the ln (c/b) and ln (i/b) axes are at an angle of 60°, these axes are here shown as orthogonal. The field for the Manilla mudstones, Tamworth Belt, New South Wales, Australia (Durney and Kisch, 1994, fig. 12), is outlined with a thin broken line.

reorientation of phyllosilicates, either in the cleavage domains or in the microlithons, appreciable c/b fissility ratios for extremely low $I_{10Å\ (0.5°)}$ C/B* intensity ratios are to be expected.

Earlier, we have noted that samples with crenulation cleavage have somewhat lower $I_{10Å\ (0.5°)}$ C/B* ratios, but *much* lower c/b cleavage/fissility ratios than most of the samples with non-crenulation domainal cleavages. The reduced $I_{10Å\ (0.5°)}$ C/B* ratios probably reflect the good bedding-parallel fabric, enhanced by the S_1 slaty fabric, in the microlithons, rather than the nature of the crenulation cleavage. However, this fabric in the microlithons by itself would be expected to lower the $I_{10Å\ (0.5°)}$ C/B* ratios much more strongly: the rather minor amount of the reduction probably indicates that its effect is in part counterbalanced by good cleavage-parallel phyllosilicate orientation in the cleavage domains. The markedly lower c/b cleavage–fissility ratios in the crenulated samples must mean that these phyllosilicate-rich crenulation-cleavage domains contribute relatively little to the cleavage fissility. An explanation of this small contribution may lie in the partly zonal nature of the crenulation cleavage: the 'frayed' transitions of the crenulation-cleavage domains into the microlithons, with clastic micas commonly continuing through the cleavage domains at an angle of up to 25° to the cleavage, presumably lend relative toughness to the crenulation-cleavage domains.

The slate, mudstone and marl samples with closely spaced ($\leq$30 μm) domainal cleavages tend to show high values of the c/b fissility ratio for given $I_{10Å\ (0.5°)}$ C/B* intensity ratios compared to the samples showing a more widely-spaced (50–150 μm) domainal cleavage, notably those with an incipient crenulation cleavage and phyllosilicate-rich cleavage domains.

Indeed there appears to be a distinct difference between the phyllosilicate orientation–fissility morphology relationship in the samples in which the domains are mainly phyllosilicate (this includes samples with incipient crenulation cleavage), and those in which they are mainly opaques: the former tend to have low c/b fissility ratios for given $I_{10Å\ (0.5°)}$ C/B* intensity ratios; for the latter the relationship is opposite.

As an example, compare the samples from south of Linthal, Chlus (upper Urnerboden) and the upper Schächental (Z91-1 to Z91-11), all with similar mid-anchimetamorphic illite 'crystallinities'. Z91-1, Z91-2A, Z91-2B, Z91-8 and Z91-9 show incipient crenulation cleavages with distinct cleavage-parallel phyllosilicate reorientation in the smooth cleavage domains spaced some 50–100 μm, and deflection towards this orientation in the outer adjoining microlithon margins (in part 'zonal' crenulation cleavage): this fabric is reflected in low c/b fissility ratios for their $I_{10Å\ (0.5°)}$ C/B* intensity ratios (the same holds for Z91-4, but here the cleavage domains are restricted to a subordinate thin bed). In contrast, the continuous S_2 crenulation-cleavage domains of Z91-3 essentially consist of opaques without phyllosilicate re-orientation, resulting in a high c/b fissility ratio, while Z91-6, Z91-7 and Z91-11 have very closely spaced ($\approx$20 μm) cleavage domains resulting in high c/b fissility ratios for the already high $I_{10Å\ (0.5°)}$ C/B* intensity ratios reflecting the advanced phyllosilicate orientation in both the cleavage domains and the microlithons (almost complete in Z91-7).

Illite–chlorite ratios

These crenulated slates are rich in mica–chlorite 'stacks', which supports the view that the earlier-noted high $I_{10Å}/I_{7Å}$ C/B ratios found in some of these at least in part reflect the growth of chlorite in the bedding-parallel mica–chlorite 'stacks'. The predominantly chloritic composition of many of the stacks suggests chloritization of clastic biotite rather than (or in addition to) chlorite growth in the voids between flakes of extended clastic white mica as the predominant process of formation of this chlorite (cf. White *et al.*, 1985; Dimberline, 1986; Li *et al.*, 1996; Ho *et al.,* 1995).

Differences in orientation of mica and chlorite have been noted in X-ray texture goniometry studies of incipient cleavage, for instance in the mudstone-to-slate transition in the Martinsburg Formation at Lehigh Gap, Pennsylvania (Holeywell and Tullis, 1975; Ho *et al.*, 1995) at high-anchizone grade (Wintsch *et al.*, 1991): in the mudstone zone, the mica basal planes are parallel to the bedding, whereas the preferred orientation of the chlorite is up to 30° shallower than the bedding; this angular difference between chlorite and mica decreases towards the transition zone, where their preferred orientations are intermediate to cleavage and bedding. In contrast, Ishii (1988) found that, beyond a metamorphic grade of IC = 0.29, chlorite showed a *better* cleavage-parallel orientation than illite. In a prograde slate sequence from Central Wales, Ho *et al.* (1996) found that at the lower grades the preferred orientation of mica and chlorite were similar; in the higher grades, anchizone and epizone, the preferred orientations of mica were mainly in the cleavage orientation, whereas those of chlorite were largely parallel to bedding. They concluded that growth of minerals in the cleavage orientation in the higher-grade samples is dominated by the dissolution and neocrystallization of mica.

The 'higher-grade' samples with $IC_{<2\ \mu m} < 0.36° \Delta 2\Theta$ that show high $I_{10Å}/I_{7Å}$ C/B ratios—i.e. much higher $I_{10Å}/I_{7Å}$ ratios in the C- than the B-slab—at increased $I_{10Å\ (0.5°)}$ C/B* ratios either contain chlorite-predominant mica–chlorite stacks, or show strong reorientation of clastic mica in the cleavage direction. These high ratios could therefore reflect either or both the following relative tendencies: (1) increase in the formation of cleavage-parallel mica or

in the preferential re-orientation of mica in the cleavage direction; and (2) increase in the formation of bedding-parallel chlorite during cleavage development, specifically the growth of chlorite on clastic mica during formation of chlorite–mica 'stacks'.

Degree of tectonic fabric development and initial bedding/cleavage fissility ratio

The fact that most of the i/b intersection/bedding ratios plot in a roughly I-constant band parallel to the c/b axis suggests that the tectonic deformation style that gave rise to these cleavages was essentially similar, with similar strong initial bedding anisotropies of $c_0/b_0 = 0.2$.

However, the i/b ratios for the crenulated samples from the Linthal–Urnerboden–Schächental area (from 2 to 5) are rather smaller than for most of the other samples. *If* the tectonic deformation style that gave rise to these crenulation cleavages was the same as for the more 'penetrative' cleavages, and the initial anisotropies were similar, then the tectonic deformation that gave rise to these crenulation cleavages must have been weaker than for the more 'penetrative' cleavages. This difference accords with the crenulation cleavages being second-generation S_2 cleavages, whereas the 'penetrative' cleavages are largely S_1 cleavages. However, the crenulation cleavages were observed to have been superimposed on an earlier, largely bedding-parallel, slaty fabric, presumably having a high initial bedding-parallel anisotropy. A higher initial bedding-parallel anisotropy for the crenulated samples would require a different tectonic style for the deformation that gave rise to the crenulation cleavage, for instance more alike to the non-plane fissility-fragment loci N_1 and N_2 in Durney and Kisch (1994, fig. 8B), rather than a weaker tectonic deformation. This could be suggested by the flatter slope of the band occupied by the points for the crenulated samples alone (Fig. 9), which projects back to a very high initial bedding/cleavage fissility ratio b_0/c_0—'b_0' in this case representing $(S_0 + S_1)_0$, and 'c_0' representing $(S_2)_0$. However, the small amount of data at hand do not allow a choice between these two possibilities.

CONCLUSIONS

The c/b fissility ratio and the $I_{10Å\ (0.5°)}$ C/B* ratio, respectively, represent the intensity of cleavage fissility relative to bedding fissility, and the overall degree of cleavage-parallel relative to bedding-parallel phyllosilicate orientation. Both are parameters of relative cleavage intensity, but they do not express exactly the same attributes of cleavage. The departure from a linear relationship between these two parameters can therefore provide useful indications of the type of incipient cleavage fabric developed, and help in detecting the presence of an earlier cleavage, while the differences in the $I_{10Å}/I_{7Å}$ C/B ratios provide information as to the relative formation of illite and chlorite during formation of the cleavage fabric in the cleavage domains and in the chlorite–mica 'stacks'.

The scatter in a plot of the c/b fissility ratio against the $I_{10Å\ (0.5°)}$ C/B* ratio for a series of samples of Tertiary flysch from the Helvetic zone of the Swiss Alps is markedly reduced when subgroups of samples with different lithology and microstructure are considered separately.

1. The siltstones and very fine sandstones and samples with a pronounced lithological bedding inhomogeneity show a much slower increase of the c/b fissility ratio with the $I_{10Å\ (0.5°)}$ C/B* ratio than do the slaty shales, mudstones and marls.
2. The samples with anchimetamorphic and 'diagenetic' illite 'crystallinity' values show rather similar relationships.
3. The samples with crenulated and the non-crenulated microfabrics show similar increases of the c/b fissility ratio with the $I_{10Å\ (0.5°)}$ C/B* ratios; however, the samples with crenulation cleavage have somewhat lower $I_{10Å\ (0.5°)}$ C/B* ratios and *appreciably* lower c/b cleavage/fissility ratios than the samples with non-crenulation domainal cleavages. As the crenulation cleavage in these samples was superimposed on an earlier slaty-cleavage fabric, this difference reflects the enhancement of the bedding-parallel phyllosilicate orientation by persistence of this earlier, largely bedding-parallel fabric in the microlithons of the crenulated, but not of the non-crenulated samples. The crenulation-cleavage domains also show wider spacings (50–150 μm) than the cleavage domains in most of the non-crenulated samples (< 30 μm).
4. There is a distinct tendency for the illite/chlorite ratio to be somewhat lower in the C slab that in the B slab in the incipient development of phyllosilicate orientation, but to markedly increase with increasing phyllosilicate orientation, so as to be almost uniformly higher when the $I_{10Å\ (0.5°)}$ C/B* ratio exceeds unity. The strong increase in the $I_{10Å}/I_{7Å}$ C/B ratio in the 'higher-grade' samples with $IC_{<2\ \mu m} < 0.36°\Delta 2\Theta$ should reflect either or both of the following relative tendencies: (1) increase in the formation of cleavage-parallel mica or in the preferential re-orientation of mica in the cleavage direction; and (2) increase in the formation of bedding-parallel chlorite during cleavage development, specifically the growth of chlorite on clastic mica during formation of chlorite–mica 'stacks'.
5. A more extensive use of the intersection/bedding fissility ratio i/b is likely to help in assessing the effect of lithology, particularly the effect of the initial bedding anisotropy.

Acknowledgements—The author is grateful to Dr David W. Durney (Macquarie University, Australia) for joining him in collecting and measuring part of the samples in the field, and for generously sharing his extensive knowledge of the western Helvetic nappes. Dr Durney is also thanked for his constructive comments on an earlier version of this paper. The many X-ray diffraction traces were run by Mrs Esther Shani and Mrs Dida Banai. Comments by Dr Stephen Marshak and an anonymous referee greatly improved the paper.

REFERENCES

Badoux, H. and Gabus, J.-H. (1991) Atlas Géologique de la Suisse 1:25,000, Feuille 1285 Les Diablerets. (2nd ed.), Service Hydrologique et Géologique National.

Borradaile, G. J., Bayly, M. B. and Powell, C. McA. (1982) *Atlas of Deformational and Metamorphic Rock Fabrics*. Springer, Berlin.

Brückner, W., Frey, F. and Trümpy, R. (1967) Exkursion Nr. 35—Glarnerland-Klausenpass (Näfels–Linthal-Altdorf). In *Geologischer Führer der Schweiz, Heft 7—Exkursionen Nr. 31–35*, eds R. Trümpy and W. Nabholz, pp. 649–693. Schweizerische Geologische Gesellschaft/Wepf & Co., Basel.

Brückner, W. and Zbinden, P. (1987) *Geologischer Atlas der Schweiz 1:25,000*. Blatt 1192 Schächental, Schweizerische Geologische Kommission/Landeshydrologie und -geologie.

Bugnon, P.-C. (1981) Géologie des racines helvétiques dans la région de Loèche (Valais) *Bulletin de la Société Vaudoise des Sciences naturelles* **75**, (359), 202–206 (*Bulletin de Géologie, Lausanne*, No 256).

Dimberline, A. M. (1986) Electron-microscope and microprobe analysis of chlorite-mica stacks in the Wenlock turbidites, mid-Wales, U. K. *Geological Magazine* **123,** 299–306.

Durney, D. W. and Kisch, H. J. (1994) A field classification and intensity scale for first-generation cleavages. *AGSO Journal of Australian Geology and Geophysics* **15,** 257–295.

Frey, M. (1988) Discontinuous inverse metamorphic zonation, Glarus Alps, Switzerland: evidence from illite "crystallinity" data. *Schweizerische Mineralogische und Petrographische Mitteilungen* **68,** 171–183.

Frey, M., Trommsdorf, V. and Wenk, E. (1980) Excursion no. IV—Alpine metamorphism of the Central Alps. In *Geology of Switzerland—A Guide-Book. Part B: Geological Excursions*, eds R. Trümpy, P. W. Homewood and S. Ayrton, pp. 295–316. Schweizerische Geologische Kommission/Wepf & Co., Basel.

Gray, D. R. (1977a) Morphologic classification of crenulation cleavages. *Journal of Geology* **85,** 229–235.

Gray, D. R. (1977b) Some parameters which affect the morphology of crenulation cleavages. *Journal of Geology* **85,** 763–780.

Groshong, R. H. (1988) Low-temperature deformation mechanisms and their interpretation. *Bulletin of the Geological Society of America* **100,** 1329–1360.

Ho, Nei-Che, Peacor, D. R. and van der Pluijm, B. A. (1995) Reorientation mechanism of phyllosilicates in the mudstone-to-slate transition at Lehigh Gap, Pennsylvania. *Journal of Structural Geology* **17,** 345–356.

Ho, Nei-Che, Peacor, D. R. and van der Pluijm, B. A. (1996) Contrasting roles of detrital and authigenic phyllosilicates during slaty cleavage development. *Journal of Structural Geology* **18,** 615–623.

Holeywell, R. C. and Tullis, T. E. (1975) Mineral reorientation and slaty cleavage in the Martinsburg Formation, Lehigh Gap, Pennsylvania. *Bulletin of the Geological Society of America* **86,** 1296–1303.

Ingram, R. L. (1953) Fissility of mudrocks. *Bulletin of the Geological Society of America* **64,** 869–878.

Ishii, K. (1988) Grain growth and re-orientation of phyllosilicate minerals during the development of slaty cleavage in the South Kitakami Mountains, northeast Japan. *Journal of Structural Geology* **10,** 145–154.

Kisch, H. J. (1980) Illite crystallinity and coal rank associated with lowest-grade metamorphism of the Taveyanne greywacke in the Helvetic zone of the Swiss Alps. *Eclogae Geologicae Helvetiae* **73,** 753–777.

Kisch, H. J. (1991) Illite crystallinity: recommendations on sample preparation, X-ray diffraction settings, and interlaboratory samples. *Journal of Metamorphic Geology* **9,** 665–670.

Kisch, H. J. (1994) X-ray diffraction intensity ratios of phyllosilicate reflections in cleavage- and bedding-parallel slabs: incipient development of slaty cleavage in the Caledonides of Jämtland, western central Sweden. *Revista Geológica de Chile* **21,** 253–267.

Krumm, S. and Buggisch, W. (1991) Sample preparation effects on illite crystallinity measurement: grain-size gradation and particle orientation. *Journal of Metamorphic Geology* **9,** 671–677.

Laubscher, H. and Bernoulli, D. (1980) Excursion III—Cross-section from the Rhine Graben to the Po Plain. In *Geology of Switzerland—A Guide Book. Part B: Geological Excursions*, eds R. Trümpy, P. W. Homewood and S. Ayrton, pp. 183–209. Schweizerische Geologische Kommission/Wepf & Co., Basel.

Li, G., Peacor, D. R., Merriman, R. J., Roberts, B. and van der Pluijm, B. A. (1994) TEM and AEM constraints on the origin and significance of chlorite–mica stacks in slates: An example from central Wales. *Journal of Structural Geology* **16,** 1139–1157.

Milnes, A. G. and Pfiffner, O. (1977) Structural development of the Infrahelvetic complex, eastern Switzerland. *Eclogae Geologicae Helvetiae* **70,** 83–95.

Oertel, G. (1983) The relationship of strain and preferred orientation of phyllosilicate grains in rocks—a review. In *Continental Tectonics: Structure, Kinematics and Dynamics*. eds M. Friedman and M. N. Toksöz. *Tectonophysics* **100,** 413–447.

Pfiffner, O. A. (1978) Der Falten- und Kleindeckenbau im Infrahelvetikum der Ostschweiz. *Eclogae Geologicae Helvetiae* **71,** 61–84.

Powell, C. McA. (1979) A morphological classification of rock cleavage. *Tectonophysics* **58,** 21–34.

Sorby, H. C. (1853) On the origin of slaty cleavage. *Edinburgh New Philosophical Journal* **55,** 137–149.

Spicher, A. (1980) *Tektonische Karte der Schweiz/Carte tectonique de la Suisse 1:500,000*. Schweizerische Geologische Kommission/Bundesamt für Landestopographie (Wabern).

van der Pluijm, B. A., Ho, N.-C. and Peacor, D. R. (1994) High-resolution X-ray texture goniometry. *Journal of Structural Geology* **16,** 1029–1032.

White, S. H., Huggett, J. M. and Shaw, H. F. (1985) Electron-optical studies of phyllosilicate intergrowths in sedimentary and metamorphic rocks. *Mineralogical Magazine* **49,** 413–423.

Wintsch, R. P., Kvale, C. M. and Kisch, H. J. (1991) Open-system, constant-volume development of slaty cleavage, and strain-induced replacement reactions in the Martinsburg Formation, Lehigh Gap, Pennsylvania. *Bulletin of the Geological Society of America* **103,** 916–927.